Supplementary Information for "Spot Size Engineering in Microscope-based Laser Spectroscopy"

P. Hauer

The MacDiarmid Institute for Advanced Materials and Nanotechnology, School of Chemical and Physical Sciences, Victoria University of Wellington, PO Box 600, Wellington 6140, New Zealand

J. Grand

Université Paris Diderot, Sorbonne Paris Cité, ITODYS, UMR CNRS 7086, 15 rue J-A de Baïf, 75205 Paris Cedex 13, France

A. Djorovic

The MacDiarmid Institute for Advanced Materials and Nanotechnology, School of Chemical and Physical Sciences, Victoria University of Wellington, PO Box 600, Wellington 6140, New Zealand

G. R. Willmott

The MacDiarmid Institute for Advanced Materials and Nanotechnology, Departments of Physics and Chemistry, University of Auckland, Auckland 1010, New Zealand.

E. C. Le Ru

*The MacDiarmid Institute for Advanced Materials and Nanotechnology, School of Chemical and Physical Sciences, Victoria University of Wellington, PO Box 600, Wellington 6140, New Zealand**

* Eric.LeRu@vuw.ac.nz

S.I. SPREADSHEETS FOR GAUSSIAN BEAM CALCULATIONS

An Excel workbook is provided as supplementary file. It contains five spreadsheets to carry out Gaussian beam calculations on standard configurations. The first three relate to

- Focusing of a Gaussian beam by a single lens.
- Focusing of a Gaussian beam by a train of two lenses, with in mind the configuration studied in the manuscript of a BFPL followed by an objective lens.
- Focusing of a Gaussian beam by a train of three lenses, with in mind the configuration studied in the manuscript of a two-lens BFP-BE combination followed by an objective lens.

The two additional spreadsheets are almost identical to the latter two, but are specifically set-up to find the parameters satisfying the condition $\Delta = 0$ (for case **B** of the manuscript) using the built-in solver in Excel. In the BFPL case, this is achieved by varying the BFPL position. In the BFP-BE case, this is achieved by varying the distance between the two lenses of the BE. As evident in the screen shot shown in Fig. S1, those spreadsheets are self-explanatory and contain a diagram defining all parameters. The orange cells can be modified. The most commonly studied outputs are indicated as green cells.

S.II. EXPERIMENTAL SETUP

A Labram HR UV Raman spectrometer (see schematic in Fig. S2) from Horiba Jobin-Yvon was used for all experimental measurements. It is suitable for micro-measurements as it is attached to a Olympus BX41 Microscope, which is equipped with an objective revolver and a CCD camera for sample viewing. The sample position can be adjusted with sub-micrometer precision through a motorized xy-translation stage. Due to space constriction, the BFPL or the two-lens BFP-BE combination have to be positioned in the small region shown in Fig. S3.

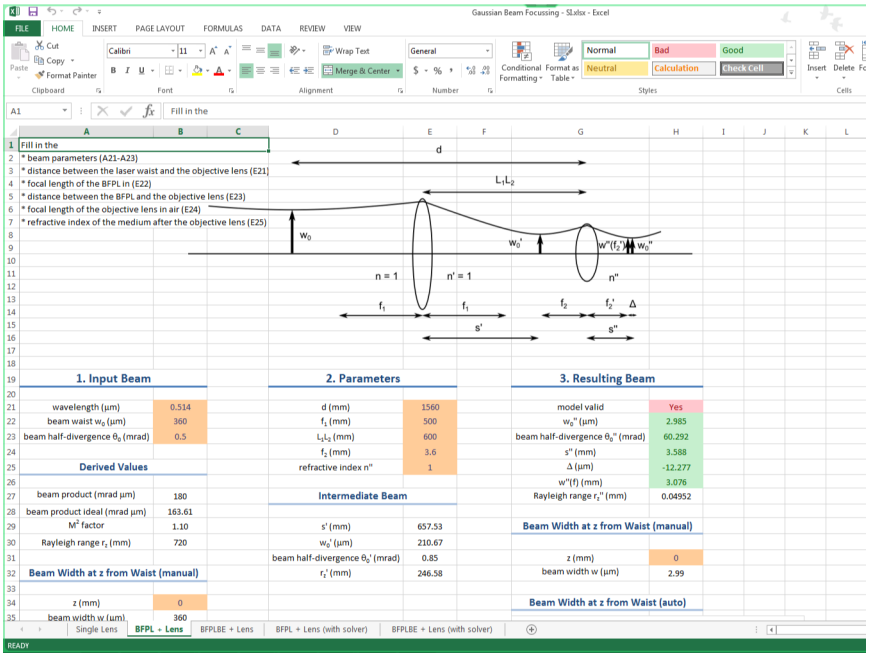

FIG. S1. Screen shot from the Excel spreadsheet modelling the BFP-BE combination.

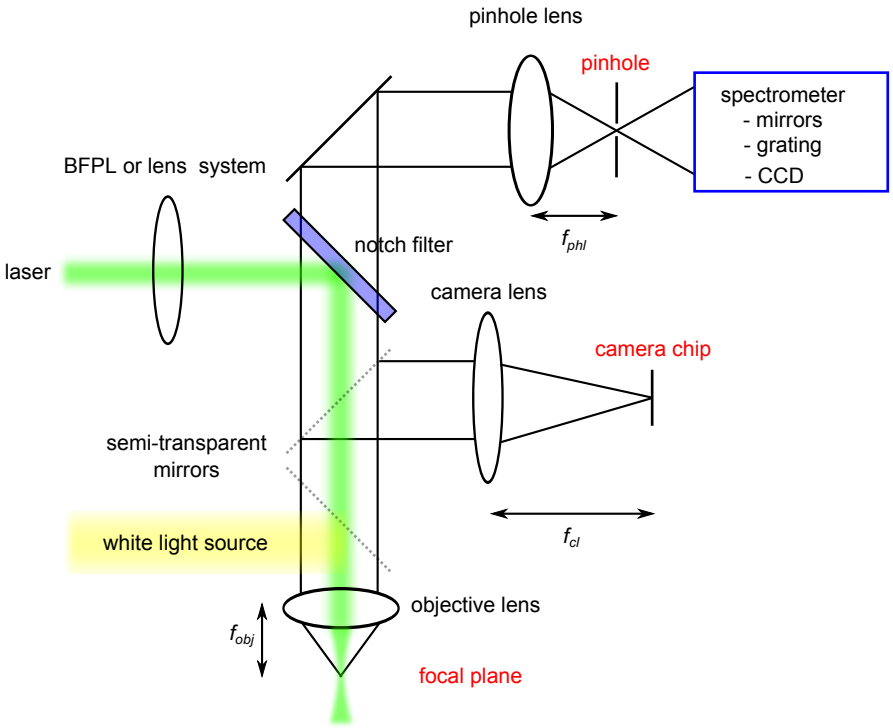

FIG. S2. A schematic layout of our Raman spectrometer. Components in red are conjugated with each other.

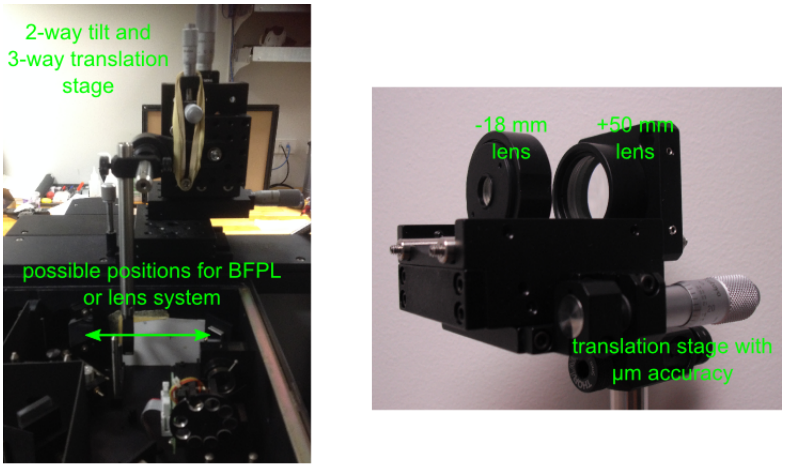

FIG. S3. (a) Installation of a BFPL in our system. The available space is limited to $\sim 15\,\mathrm{mm}$ of the optical beam path, no closer than 600 mm from the objective. (b) The two lenses used in the BFP-BE system are mounted in a contraption to tune the distance between them with μm precision.

S.III. MEASURING Δ, DISTANCE BETWEEN OBJECTIVE AND LASER FOCUS

Measuring the distance between the focal plane of the objective and laser focus appears to be a trivial task. The sample is illuminated both with a white light source and the laser and viewed with a camera and the positions on the vertical adjustment of the microscope table where the sample appears in focus ("white light focus") and where the laser appears to have the smallest size ("apparent laser focus") are noted. However, the position at which the laser spot appears minimal ("apparent laser focus") *does not* coincide in general with the actual position of the beam waist of the focused laser ("real laser focus"). This appears counter-intuitive at first, and it will also depend on the nature of the sample. In our case, we used a highly (specular) reflective sample (silicon). Such a sample creates an image of the incident Gaussian beam, and this image is centered at the mirror image position of the incident beam center. As a result, if the distance from the "white light focus" to the "real laser focus" is Δ (by definition of Δ), then the distance from the "white light focus" to the "apparent laser focus" is in fact $\Delta/2$ (see Fig. S4).

This can be further described by accounting for the way the image is created at the

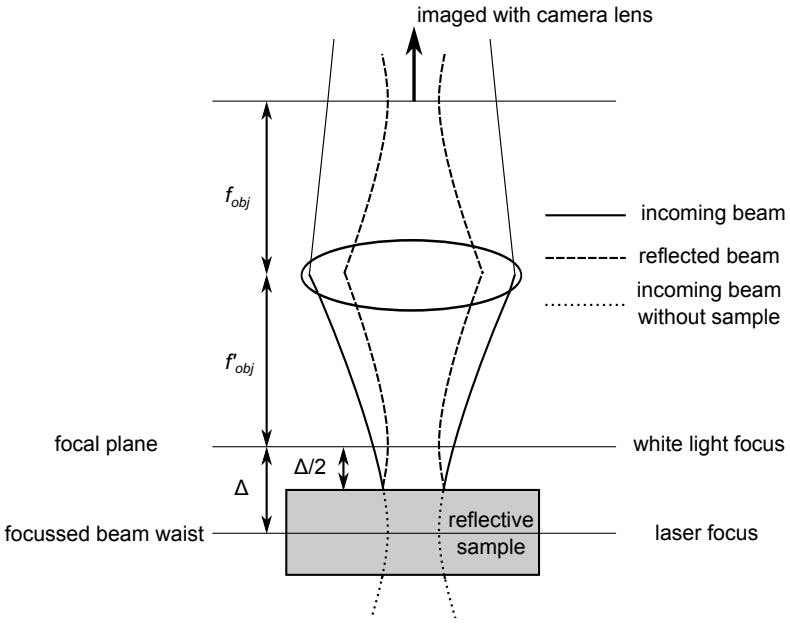

FIG. S4. The incoming an reflected beam when using a highly specular reflective sample.

camera CCD (see Fig. S4). The light collected by the objective is focused onto a camera chip, positioned at the focal plane of the camera lens. As the camera chip is positioned at the focal plane of the camera lens, the beam width at the focal plane is, according to Self's formalism, $\theta'_0 f_{cl}$. The smallest possible spot size is therefore achieved when θ'_0 becomes minimal, which is equivalent to w'_0 being maximum. As the position and size of the incident beam is constant, this occurs when the mirror image of this beam waist is in the focal plane of the objective. The image of the laser spot viewed with such a camera is minimal when the sample is positioned at half the distance between the focal plane of the objective and the actual laser waist. This perhaps counter-intuitive result was confirmed experimentally by measuring the beam waist at different positions along the axis. In this context it has to be noted that a correct positioning of the camera lens is essential to avoid a systematic error in the measurements of Δ. This can be ensured for example by checking that the "white light focus" remains at the same location within a few micrometers when the magnification of the used objective (from the same manufacturer) is changed.

If instead a diffusively reflecting sample is used, the reflected light can be understood as a superimposition of point sources, for which geometric optics can be used. Taking the rays of the collected path into account the position of the "apparent laser focus" will then coincide with the 'white light focus". The "real laser focus" can not be determined in this case.

S.IV. ADDITIONAL DETAILS ON THE BFPL AND BFPL-BE CONFIGURATIONS

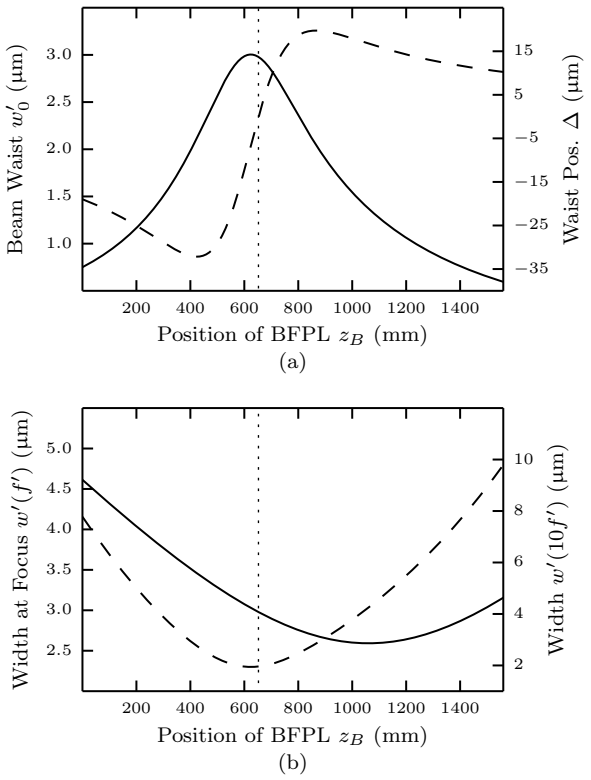

FIG. S5. (a) The size of the beam waist (—) and its position (- -) as a function of the lens distance when a BFPL with $f_B = 500\,\text{mm}$ and an objective lens with focal length 3.6 mm are used. Negative values indicate that the beam waist is located closer to the lens than its focal plane. Note that in order to achieve $s' = f'$, the required distance (vertical line) is not exactly equivalent to the maximum beam waist, which is achieved at a slightly shorter distance. (b) The beam width at the objective focus (—) and at a distance $10f'$ (- -) from the objective lens.

In the BFPL configuration, the spot size and the position of the focused beam waist are quite sensitive to the exact BFPL position (Fig. S5 (a)). Experimentally the correct position for the BFPL can be found by observing the beam beyond the focal plane of the objective lens, where the laser spot is already significantly wider and can easily be viewed by eye (for example at a distance ten times the focal length of the objective lens). By moving the BFPL forward and backward, the optimum position can be found by minimizing the

spot size there (which is equivalent to minimizing the beam divergence). This way, one will achieve a situation which does not exactly result in $s' = f$ but is close enough for most purposes. By simply observing the spot in the focal plane one would not be able to find the correct position of the BFPL as the size of the beam width depends approximately linearly on the distance between the lenses close to the critical position (Fig. S5 (b)). This, however, is also of advantage as the spot size at the focal plane, which is the relevant parameter in most experiments, is relatively insensitive and also tunable with the position of the BFPL.

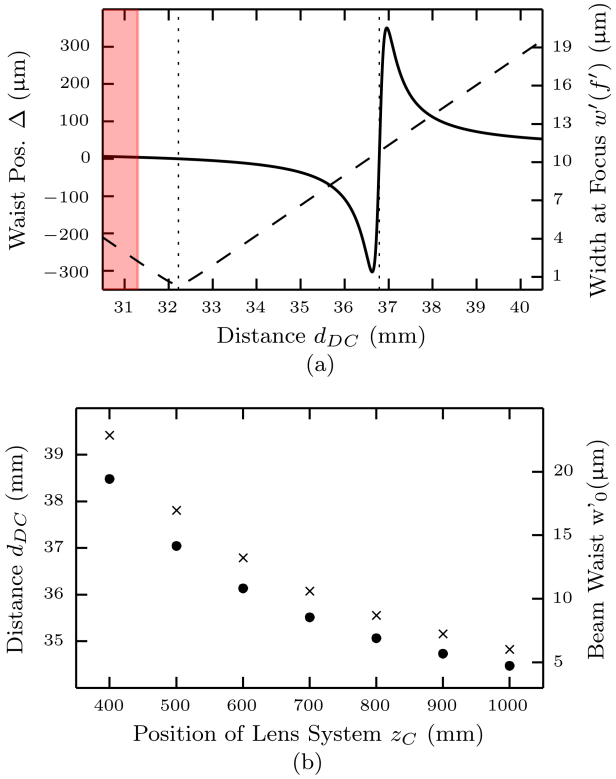

FIG. S6. (a) Predicted offset Δ solid line, left axis) and beam width at the focal plane $w'(f')$ (dashed line, right axis) as a function of the distance $|d_{DC}|$ between the two lenses of the BFP-BE combination using a fixed BFP-BE-to-objective distance of $|z_C| = 600\,\text{mm}$ and a $\times 50$ objective. The shaded area indicates that the paraxial assumption is no longer valid. The vertical dotted lines indicate where $\Delta = 0$. (b) The required distance $|d_{DC}|$ (crosses, left axis) between the two lenses of the BFPL-BE in order to achieve the situation in case **B** ($\Delta = 0$) and the resulting beam waist (circles, right axis) as a function of the the BFP-BE-to-objective distance z_C.

In the BFP-BE configuration, the correct distance $|d_{DC}|$ between the two lenses that

fulfills the condition $\Delta = 0$ (case **B**) and produces the largest spot size can be found experimentally in a similar fashion as explained above. To achieve the smallest spot size, i.e. use the lens combination as an actual beam expander, $|d_{DC}|$ has to be adjusted to the distance where the spot size appears minimal when observing the spot through the objective (Fig. S6 (a)). When the constraint $|z_C|$ =constant is lifted, the spot size can be continuously tuned over a wide range while retaining the condition $\Delta = 0$ by adjusting $|d_{DC}|$ accordingly (Fig. S6 (b)).

S.V. SUPPLEMENTARY METHODS: SAMPLE PREPARATION FOR FLUORESCENCE

The Rhodamine B dye monolayer was prepared according to the following modification of the procedure introduced by Tawde et al. [1]. A self-assembled monolayer of phenylsilane was first deposited onto a clean, pre-prepared, hydrophilic quartz substrate. A 2 mM solution of trichlorophenylsilane (Sigma Aldrich, $\geq$ 97%) in a 7:6 (volume-volume ratio) toluene/chloroform mixture was prepared in a beaker under a nitrogen atmosphere. After this initial silanization of the glass beaker walls, the solution was discarded and re-made in the same beaker to preserve a well-defined silane concentration. Note that both the toluene and chloroform need to be anhydrous due to the high reactivity of trichlorophenylsilane with water. The silane film was deposited by dipping the quartz substrate into the prepared silane solution for 10 mins under sonication and then left to stand in the solution for a further 45 minutes. The substrate was then removed, dried with a jet of nitrogen and cured for 15 minutes at 50°C. The substrate was then left to cool for 15 minutes then dipped into a beaker with a 100 μM solution of Rhodamine B in deionised water (Ultrapure MilliQ). The beaker was then covered with Parafilm and left to stand 24 hours, upon which the substrates were removed from solution and the excess dye was washed off by rinsing with deionised water then patted down with a Kimwipe. The backside of the films was cleaned with toluene to remove any adsorbed silane and Rhodamine B. The prepared films show a very light pink

color.

---

[1] S. R. Tawde, D. Mukesh, J. V. Yakhmi, and C. Manohar, "Dye adsorption on self-assembled silane monolayers: optical absorption and modelling," J. Mat. Chem. **9**, 1847–1851 (1999).